FEATURE ARTICLE

ChemComm
www.rsc.org/chemcomm

Controlling chemistry with cations: photochemistry within zeolites

V. Ramamurthy,*[a] J. Shailaja,[a] Lakshmi S. Kaanumalle,[a] R. B. Sunoj[b] and J. Chandrasekhar[b]
[a] *Department of Chemistry, Tulane University, New Orleans, LA, USA 70118*
[b] *Department of Organic Chemistry, Indian Institute of Science, Bangalore, India 560 012*

Received 2nd January 2003, Accepted 26th March 2003
First published as an Advance Article on the web 9th July 2003

The alkali ions present in the supercages of zeolites X and Y interact with included guest molecules through quadrupolar (cation-π), and dipolar (cation–carbonyl) interactions. The presence of such interactions can be inferred through solid-state NMR spectra of the guest molecules. Alkali ions, as illustrated in this article, can be exploited to control the photochemical and photophysical behaviors of the guest molecules. For example, molecules that rarely phosphoresce can be induced to do so within heavy cation-exchanged zeolites. The nature (electronic configuration) of the lowest triplet state of carbonyl compounds can be altered with the help of light alkali metal ions. This state switch (nπ*–ππ*) helps to bring out reactivity that normally remains dormant. Selectivity obtained during the singlet oxygen oxidation of olefins within zeolites illustrates the remarkable control that can be exerted on photoreactions with the help of a confined medium that also has active sites. The reaction cavities of zeolites, like enzymes, are not only well-defined and confined, but also have active sites that closely guide the reactant molecule from start to finish. The examples provided here illustrate that zeolites are far more useful than simple shape-selective catalysts.

V. Ramamurthy (M.Sc, IIT Madras; Ph.D, University of Hawaii) had his postdoctoral training in the laboratories of P. de Mayo (University of Western Ontario) and N. J. Turro (Columbia University). Prior to joining Tulane in 1994 he was on the faculty at the Organic Chemistry Department, Indian Institute of Science, Bangalore (1978–87) and Central Research, The Du Pont Company (1987–1994). His main research interests have been on understanding the excited state behavior of organic molecules in confined media (crystals, micelles, cyclodextrins and zeolites).

J. Shailaja (M.Sc, University of Madras) having obtained Ph.D. degree from Tulane University is currently carrying out postdoctoral work in the laboratory of D. L. Gin (University of Colorado).

L. S. Kaanumalle having completed her M.Sc at IIT Madras is currently carrying out research on asymmetric photochemistry at Tulane University towards her Ph.D. dissertation.

R. B. Sunoj (M.Sc, University of Kerala) obtained his PhD degree from the Indian Institute of Science, Bangalore under the supervision of J. Chandrasekhar. Following postdoctoral work with C. M. Hadad (Ohio State University) he is currently on the faculty at the Indian Institute of Technology, Bombay.

J. Chandrasekhar (M.Sc., Ph.D., IIT Madras) carried out postdoctoral research in the groups of P.v.R. Schleyer (Erlangen, Germany) and W. L. Jorgensen (Purdue University, USA) and was a faculty in the Department of Organic Chemistry, Indian Institute of Science, Bangalore. Currently, he is a Research Fellow at Neurogen Corporation (Branford, CT). His research interests have focussed on developing and using computational models for solving diverse chemical problems.

Introduction

Physical features such as the size of the reaction vessel can be ignored in reactions carried out in vessels disproportionately larger than the reactant molecule. However, in reactions where the reactant molecule and the reaction vessel are nearly of the same size, these factors acquire significant importance.[1] Thus, by controlling the size, shape and active sites of the reaction vessel, one should be able to control what occurs within a confined space ('reaction cavity').[2] Two striking photobiological phenomena which illustrate what can be achieved in a confined environment are photosynthesis and visual signal transduction. In the former, the medium (protein) is able to organize a number of active elements so as to predispose them to a desired physical process, while in the latter, the medium (rhodopsin) restricts the rotational mobility on certain parts of a single molecule, retinal. These, as well as the remarkable selectivities exhibited by enzymes, have driven chemists to examine various confined media in pursuit of selectivity.

In this article we make use of zeolites that are similar in composition to glass and quartz vessels as reaction media. Silicon, aluminum and oxygen atoms, the inert components of the photochemical macromolecular reactors like quartz or Pyrex vessels, when used as molecular sized enclosures (zeolites) of a substrate, are capable of influencing its reactivity. 'Shape selectivity' is a key concept applied in many of the chemical processes involving zeolites as media or as reagents.[3] In this context zeolites may be viewed as possessing reaction cavities of fixed size and shape, and selectivity is achieved by matching these characteristics of the zeolite to those of products and/or transition states. However, the supercages of zeolites X and Y, as described below, contain a large number of cations that have been established to interact with the included guest molecules. These cation–guest interactions utilized in industrial scale gas separations are seldom used to control chemical reactions.[4] Similarly to enzymes, zeolites have well-defined reaction cavities and active sites (cations), which could help to steer reactions towards a single pathway.[5] Exploitation of alkali metal ion–organic interaction, in addition to shape selectivity, as illustrated in this article, could result in far higher and newer types of selectivities. For such purposes as chemical reaction control, zeolites may be viewed as polyelectrolytes with 'porous salt-like structures' with sufficient empty space to accommodate organic molecules. Knowledge of factors controlling the molecular structure of a guest within a zeolite would facilitate the use of zeolites as media for performing selective

DOI: 10.1039/b212741e

chemistry of included molecules from all three phases (gas, liquid and solid).

Zeolites in general may be regarded as open structures of silica with aluminum substitution in a well-defined fraction of the tetrahedral sites. The framework thus obtained contains pores, channels and cages of different dimensions and shapes. The partial substitution of trivalent aluminum ions for the tetravalent silicon ions at lattice positions results in a network that bears a net negative charge which is compensated by exchangeable positively charged counter ions. Both X and Y zeolites are used as reaction media in this study.[6] The topological structure of X- and Y-type zeolites (faujasites) consist of an interconnected three-dimensional network of relatively large spherical cavities, termed supercages (diameter of about 13.4 Å; Fig. 1). Each supercage is connected

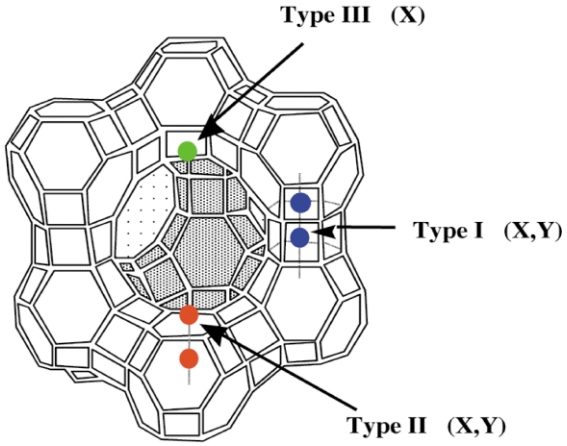

Fig. 1 Structure of the supercage in zeolites X and Y. Position of cations are indicated as Types I, II and III.

tetrahedrally to four other supercages through 7.6 Å windows or pores. The charge-compensating cations present in the internal structure of X and Y zeolites are known to occupy three different positions; the first type (site I), with 16 cations per unit cell (both X and Y), is located on the hexagonal prism faces between the sodalite units. The second type (site II), with 32 per unit cell (both X and Y), is located in the open hexagonal faces. The third type (site III), with 38 per unit cell in the case of X type and only eight per unit cell in the case of Y type, is located on the walls of the larger cavity. Only cations at sites II and III are expected to be readily accessible to the organic molecule adsorbed within a supercage. A number of physical characteristics such as the electrostatic potential and electric field within the cage, the spin–orbit coupling parameter and the space available for the guest within the supercage are altered by the exchangeable charge compensating cations.

Switching electronic spin with alkali metal ions through alkali metal ion–organic weak interaction (spin-orbit coupling)

The intersystem crossing (ISC) of the excited molecule from S_1 to T_1 is the most important process of interest for the current discussion. The rules for ISC suggest an indirect correlation between the rate and the electronic configuration of the two states involved, *i.e.*, a faster rate with different electronic configuration ($n\pi^*$ and $\pi\pi^*$) and slower rate with the same electronic configuration ($\pi\pi^*$ and $\pi\pi^*$ or $n\pi^*$ and $n\pi^*$).[2] Thus aromatics ($\pi\pi^{*1}$ to $\pi\pi^{*3}$), olefins ($\pi\pi^{*1}$ to $\pi\pi^{*3}$) and azo compounds ($n\pi^{*1}$ and $n\pi^{*3}$) have low ISC rate, poor ISC quantum yields, rarely phosphoresce and react from T_1 upon direct excitation. The importance of spin-orbit coupling in ISC process has been well established.[7] As summarized in Table 1 the spin-orbit coupling parameter of the alkali ion increases with the atomic number. We show here a zeolite exchanged with different heavy alkali metal ions to be a powerful matrix to

Table 1 Estimated Spin-Orbit Coupling Constants for Metal Ions [a]

Zeolite	Spin-orbit coupling constant for the corresponding atom ζ/ cm^{-1}	Zeolite	Spin-orbit coupling constant for the corresponding atom ζ/ cm^{-1}
LiY	0.23	RbY	160
NaY	11.5	CsY	370
KY	38	TlY	3410

[a] Values are taken from *Handbook of Photochemistry*, S. L. Murov, I. Carmichael and G. Hug,Marcell Dekker, New York, 1993, pp. 338–341. The numbers for the corresponding ion are expected to be different but we expect the trend to remain the same.

observe phosphorescence from even those organic molecules that do not phosphoresce under normal conditions. The potential of this technique is shown with three classes of molecules namely aromatics, polyenes and azo compounds.

As shown in Fig. 2, the emission spectrum of naphthalene is profoundly affected by inclusion in faujasites.[8] For low-mass

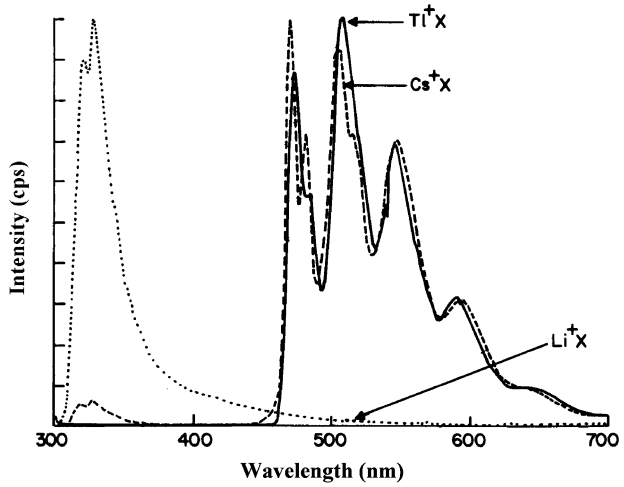

Fig. 2 Emission spectra at 77K of naphthalene included within LiX, CsX and TlX. Note the difference in relative intensities of fluorescence and phosphorescence with the cation. In LiX essentially fluorescence and in TlX essentially phosphorescence is observed.

cations such as Li^+, the emission spectra show the typical naphthalene blue fluorescence. However, as the mass of the cation increases (*e.g.*, from Li^+ to Cs^+ to Tl^+), there is a dramatic decrease in fluorescence intensity and a simultaneous appearance of the phosphorescence of naphthalene. Support for the heavy alkali metal ion enhancement of phosphorescence is evident from the dependence of the ratio of fluorescence to phosphorescence on the Cs^+ to Na^+ content in a zeolite. As seen in Fig. 3, the phosphorescence intensity of phenanthrene increases with the Cs^+ ion content. The general nature of the above is reflected by results with other aromatic compounds. Heavy-atom induced phosphorescence which allows the use of optical detection of magnetic resonance (ODMR) in zero applied magnetic field has provided information on the geometry of the alkali metal ion–aromatic (naphthalene) interaction in zeolites.[9] The sublevel specific dynamics for adsorbed naphthalene show a distinct increase in relative radiative character and total rate constant of the out-of-plane x-sublevel with increasing mass of the cation perturber. ODMR kinetic results suggest naphthalene to be adsorbed through its π-cloud at a cation site (cation-π-interaction).

The uniqueness of such use of zeolites is the ability to observe phosphorescence from systems, which commonly fail to show this emission in organic glassy matrices even when subjected to heavy atom effect. Olefinic systems that under normal conditions do not show phosphorescence emit from their triplet states at 77K when included in Tl^+-exchanged zeolites. We have

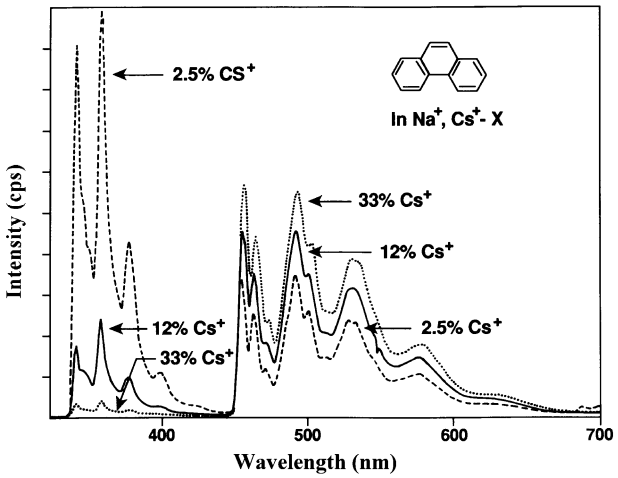

Fig. 3 Emission spectra at 77K of phenanthrene included within CsNaX zeolite at 77K. Note the intensity of phosphorescence increases with the increase in Cs^+ content.

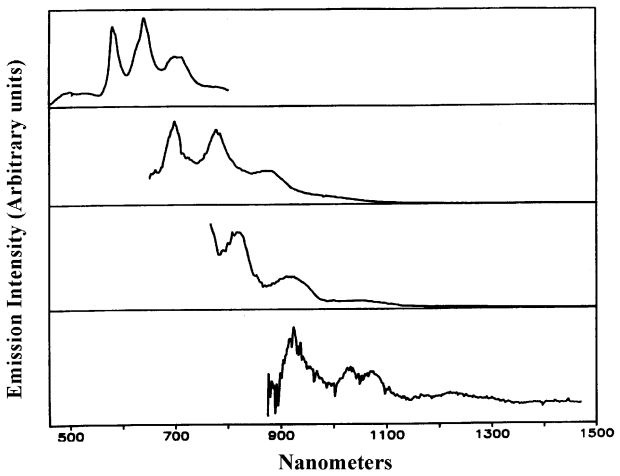

Fig. 4 Phosphorescence spectra at 77K of all *trans*-diphenylpolyenes (from top to bottom: stilbene, 1,4-diphenylbutadiene, 1,6-diphenylhexatriene, 1,8-diphenyloctatetraene) included within Tl^+ZSM-5.

succeeded in recording phosphorescence from all-*trans*-α,ω–diphenylpolyenes which commonly exhibit very low inter-system crossing efficiencies and efficient fluorescence, by including them in Tl^+-exchanged zeolites (Fig. 4).[8,9]

Results obtained with azo compounds support our expectation that a zeolite could also influence ISC between a nπ* singlet and a nπ* triplet. Numerous studies on azo compounds have established them to possess very poor ISC and not phosphoresce at 77K even in the presence of a heavy atom perturber. The lack of ISC has been attributed to the presence of a large energy gap (> 15 kcal/mole) and to the nπ* character of the excited states involved in ISC. A number of azo compounds that do not phosphoresce in organic glass do so within a Tl^+Y zeolite at 77K (for an example see Fig. 5) thus supporting our expectation that a zeolite could also influence ISC between a nπ* singlet and a nπ* triplet of azo compounds.[10]

The utility of the heavy alkali ion effect in controlling product distribution in photochemical reactions as illustrated below with the three representative examples of acenaphthylene, dibenzobarrelene and dibenzylketone. Irradiation of acenaphthylene (**1**) in solution yields the *cis* and the *trans* dimers; the excited singlet gives predominantly the *cis* dimer **2**, whereas the triplet gives both *cis* and *trans* dimers in comparable amounts (Scheme 1). Photolyses of dry solid inclusion complexes of acenaphthylene in various cations (Li^+, Na^+, K^+, Rb^+)-exchanged Y zeolites gave the *cis* and *trans* dimers in varying ratios.[11] The exclusive formation of the *cis* dimer supports our conclusion that the dimerization in the supercages of LiY and NaY is from the excited singlet state. The higher yield of the *trans* dimer **3** in KY and RbY is believed to be a consequence of the heavy-atom effect caused by the alkali metal ion present within the supercage.

Dibenzobarrelenes react differently from their triplet and excited singlet states (Scheme 2).[12] Essentially 100% triplet derived product **6** was observed within TlY, while in KY the excited singlet product **5** was obtained as the major product. There is a clear trend in the triplet product contribution with the spin orbit coupling parameter of the cation (Tl^+ > Cs^+ > Rb^+ > K^+; Table 1).

The last example relates to influencing product distribution *via* spin change of a radical pair.[13] As illustrated in Scheme 3, photolysis of dibenzylketone **7** leads to the formation of benzyl and phenylacyl triplet radical pair. In the absence of geminate recombination the radical pair diffuses apart, decarbonylates, and couples to yield 1,2-diphenylethane **8**. However, with diffusional separation restraints in a medium such as zeolite the primary triplet radical pair may undergo ISC to the singlet state from where rearrangement to *ortho* and *para*-phenyl substituted

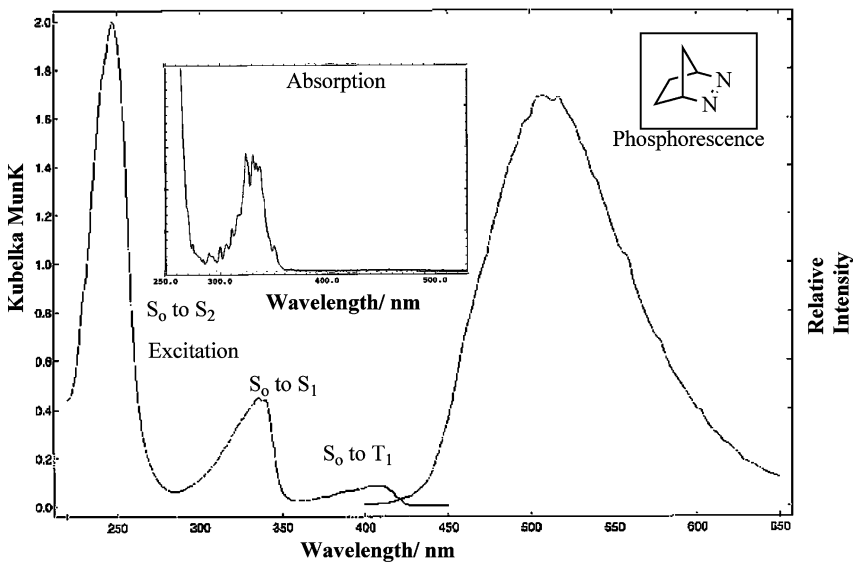

Fig. 5 Emission and excitation spectra of diazo-(2,3)-bicycloheptane included within TlY, recorded at 77K. Insert shows the diffuse reflectance absorption spectrum. The emission on the right is assigned to be phosphorescence. The longest wavelength band in the excitation spectrum is believed to be S_0 to T_1 transition.

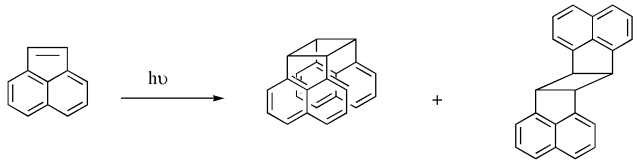

1 2 3

Zeolite	Cis/Trans
LiY	25
NaY	25
KY	2.3
RbY	1.5

Scheme 1

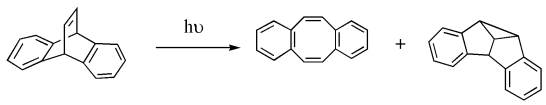

4 5 6

Scheme 2

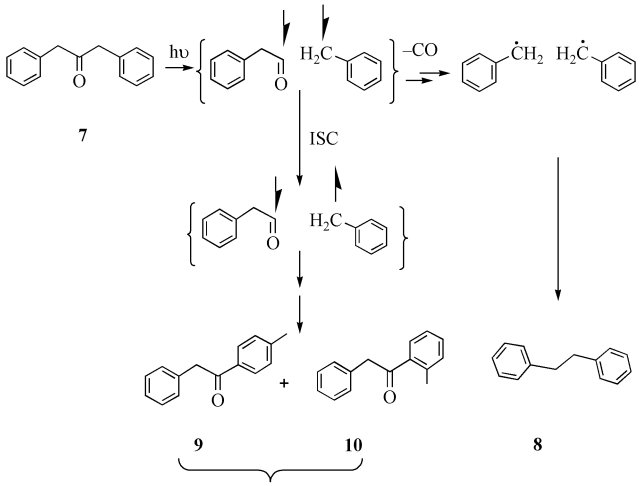

7 9 10 8

Hexane	0	>99%
KY	20	80
RbY	30	70
CsY	63	37
TlY	76	23

Scheme 3

benzophenones **9** and **10** could occur. As shown in Scheme 3, the ratio of 1,2-diphenylethane to the benzophenone derivatives within zeolites depends on the alkali ion with the lighter one favoring the former and the heavier one favoring the latter, respectively.

Switching excited state electronic configuration with alkali metal ions through alkali ion-carbonyl dipolar interaction

Molecules possessing a carbonyl chromophore have two types of lowest excited states, nπ* and ππ*.[7] In this section, we show through computational methods, solid state NMR, and steady-state and time-resolved emission experiments and product studies that the nature of the lowest triplet state of aryl alkyl ketones and cyclic enones could be controlled with the alkali ions present in zeolites.

Density functional theory calculations (B3LYP/6-31G*) suggest that Li^+ binds to acetophenone (ACP) via two modes, (a) dipolar interaction to carbonyl (mode I) and (b) cation-π interaction to phenyl ring (mode II) (Fig. 6).[14] Binding affinities

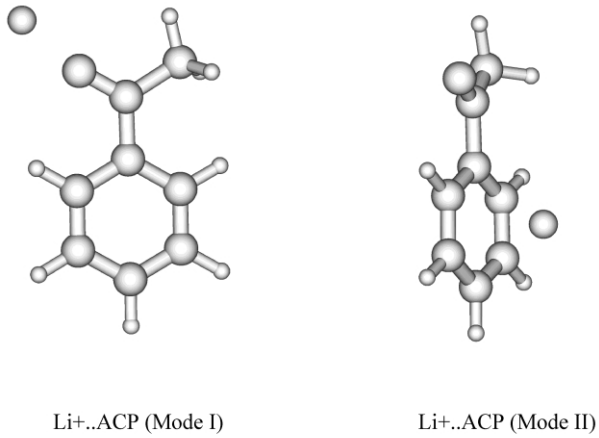

Fig. 6 B3LYP/6-31G*-Optimized geometries for the S_0 states $Li^+\cdots$ACP.

(BA) of Li^+ to ACP in these two modes in both the ground state (55.3 and 37.7 kcal/mol) and the triplet state (57.3 and 47.2 kcal/mol) are large. As would be expected, Li^+ binds more strongly (BA in ground state: 55.3 kcal/mol) than Na^+ ion (39.9 kcal/mol) to ACP. Based on the results with Li^+ and Na^+ we believe the binding affinity to follow the trend $Li^+ > Na^+ > K^+ > Rb^+ > Cs^+$.

Solid state NMR results support the computational predictions.[14] The three independent measurements, static, magic angle spectra (MAS) and cross-polarized magic angle spectra (CP-MAS) of ^{13}C-enriched ACP included in MY zeolites suggest an interaction between the alkali ion and ACP molecules: (a) The line width in the case of static and MAS spectra (Fig. 7), and signal intensity in the case of CP-MAS (Fig. 8) spectra depend on the cation (MY) suggesting lesser mobility of ACP molecules in LiY and greater freedom of movement in CsY. (b) Greater mobility of ACP molecules on silica which lack alkali metal ion than within NaY zeolites which has at least 4 type II alkali metal ions in a supercage speaks for the importance of alkali metal ion…ACP interaction. (c) From comparison of the line width in MAS spectra of ACP in NaY zeolites of varying Si/Al ratio (line width at half height: 500, 390, 350 and 300 Hz in zeolites of Si/Al ratio 2.5, 6, 15 and 40), it is obvious that ACP molecules are more restricted within NaY of high alumina content (consequently more alkali ion). For example ACP molecules are more restricted in Y zeolites with Si/Al:2.4 (line width in MAS spectra:500 Hz) than in Y zeolites with Si/Al:40 (line width in MAS spectra:300 Hz). (d) ACP molecules are more mobile within hydrated (line width in MAS spectra:140Hz) than in dry NaY.

Density functional theory calculations (B3LYP/6-31G*) employed to identify the consequence of alkali metal ion binding on the ordering of excited triplet states indicated that the ordering of the frontier molecular orbitals changes both in the ground and in the excited triplet states upon Li^+ complexation (Fig. 9).[14] Based on the orbital energies the lowest triplet state of free and Li^+ bound ACP is predicted to have nπ* and ππ* configurations. Time-dependent density functional theory calculation (TDDFT) besides correctly predicting the ordering in the case of unperturbed ACP and 4′-methoxyacetophenone (MACP), identified the triplet energies within a few kcal/mole (< 2 kcal/mol) of experimental values. Even more impressive was the fact that computed energy gaps between nπ* and ππ* states in ACP and MACP were consistent with the experimental observations (< 5 kcal/mol). Consistency between computed and experimental results with ACP and MACP gave us

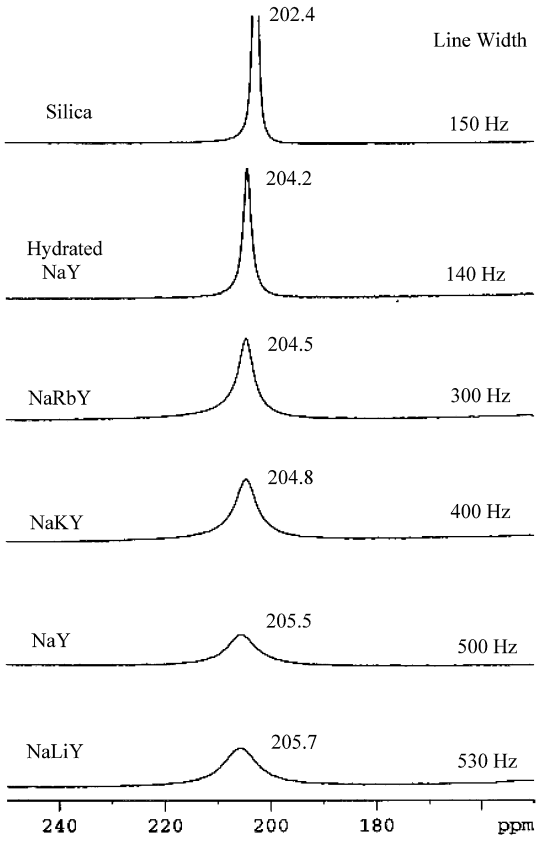

Fig. 7 MAS NMR spectra of ^{13}C (C=O) enriched acetophenone included in NaLiY, NaY, NaKY, NaRbY, hydrated NaY and silica gel. Note the variation of line width with the zeolite.

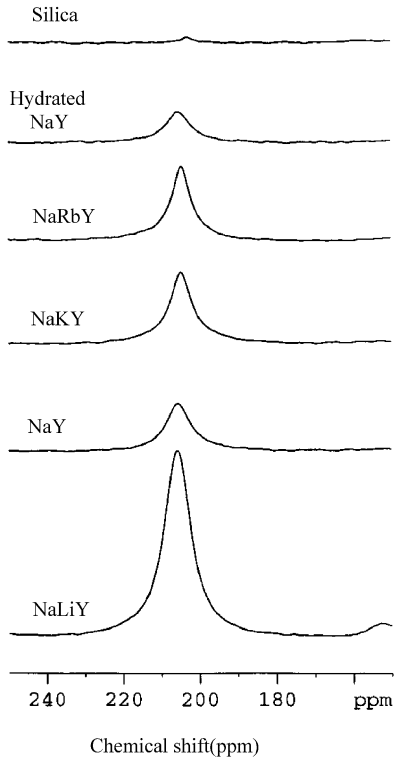

Fig. 8 ^{1}H–^{13}C CP-MAS spectra of ^{13}C (C=O) enriched acetophenone included in NaLiY, NaY, NaKY, NaRbY hydrated NaY and silica gel. Note the variation of the intensity of the signal with the zeolite.

confidence in the results obtained in the case of alkali metal ion bound ACP. Computational prediction of interest to the studies in zeolites is the lowered energy level of ππ* triplet below nπ* state when Li^+ and Na^+ bind to ACP through the carbonyl oxygen

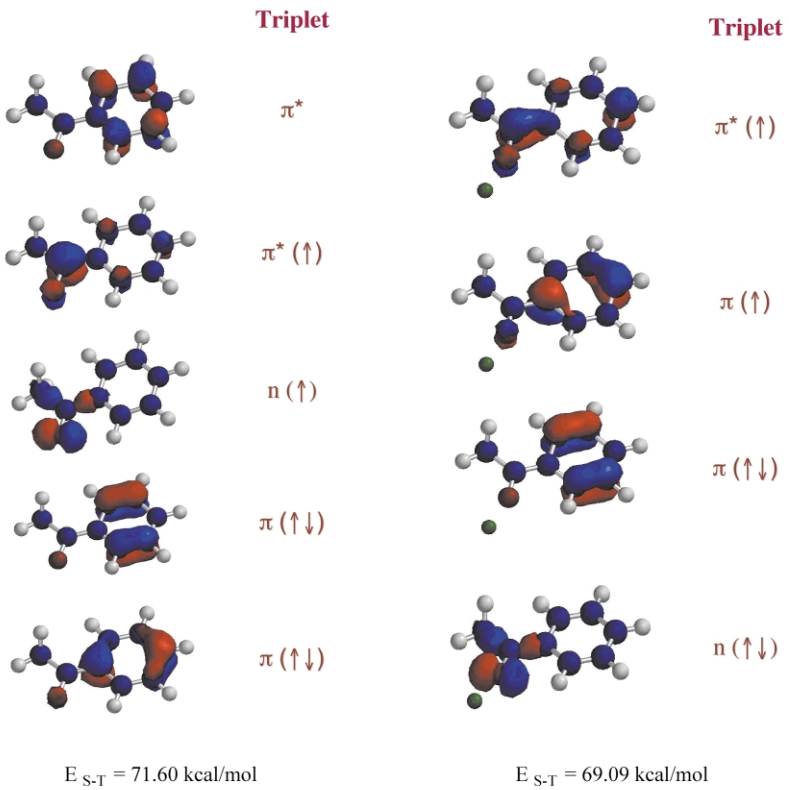

Fig. 9 Orbital diagram showing the nature of triplet excitation in the triplet state of in ACP and $Li^+\cdots$ACP (complexed to CO) computed at B3LYP/6-31G* level. Computed triplet energies of T_1 are included at the bottom.

We have used fingerprint features of nπ* and ππ* state emissions and their lifetimes to experimentally identify the nature of the lowest triplet of acetophenones included within alkali ion exchanged Y zeolites.[14] It is known that at 77K, while ACP in nonpolar as well as moderately polar organic solvents shows a structured emission (phosphorescence) with a short lifetime (msec range) characteristic of nπ* states, MACP shows a broad emission with a long lifetime (sec) characteristic of ππ* triplet state. As illustrated in Fig. 10, ACP within NaY shows, independent of the time slice, broad phosphorescence, suggesting the emitting state to be ππ* in character. Triplet lifetime measurements further confirm the ππ* character of the emitting state within NaY. The emitting state in the case of ACP-NaY has only one long component with a lifetime of 420 msec. It is important to note that the alkali metal ions that can interact strongly (Li^+, Na^+ and K^+) with the carbonyl chromophore show only ππ* like phosphorescence. The change in the nature of the lowest triplet state from ππ* to nπ* state on co-inclusion of methanol accurately identifies the source of state switch within NaY to be the binding of alkali metal ion to carbonyl (Fig. 10). Were the polarity of zeolites the causative factor for the state switch, inclusion of methanol in the zeolites, should have stabilized the ππ* state. The observed effect is consistent with our model where the binding of methanol to the alkali metal ions would release ACP to exhibit its inherent triplet nπ* character.

When Li^+ binds to ACP via the phenyl ring (mode II in Fig. 6) the lowest triplet is predicted (B3LYP/6-31G*) to have nπ* character. The observed phosphorescence emission within LiY and NaY is characteristic of ππ* state suggesting alternate binding of the cations to ACP. In fact B3LYP/6-31G* computation shows energetic preference of binding to carbonyl oxygen over the phenyl ring by 17.6 kcal/mol. Thus a comprehensive view of the results of computation, solid state NMR and photophysical studies clearly establish the source of the triplet state switching observed with ACP in MY zeolites to be due to alkali metal ion···ACP interaction via the carbonyl oxygen.

According to the CIS(D)/6-31+G* calculations, similar to ACP, the character of the lowest triplet states of cyclopentenone and cyclohexenone are also expected to switch from nπ* to ππ* due to interaction with alkali metal ions.[15] Upon irradiation of alicyclic enones within zeolites a most remarkable consequence of alkali metal ion controlled state switching can be seen in the photoproduct distributions.[16] Steroidal enones such as cholesteryl acetate (**11**) yield product **13** from nπ* triplet state in solution (Scheme 4). However, within NaY zeolite the major

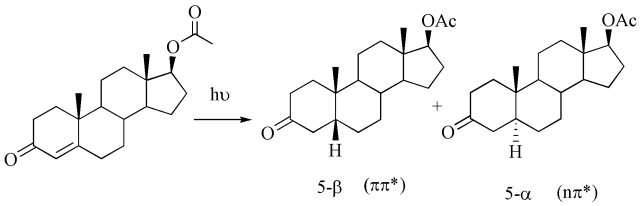

11 **12** **13**

Hexane	No reaction	
2-propanol	27 %	73 %
NaY (Si/Al: 2.5)	85	15
NaY (Si/Al: 300)	No reaction	

Scheme 4

product **12** is derived from the ππ* triplet state. Formation of the β-hydrogen insertion product **12** within zeolite is consistent with its origin from the ππ* state.[17] Androstenedione (**14**) has been established to react in solution mainly from the cyclopentanone D-ring (Scheme 5). No products due to reactions from the D-ring are seen upon irradiation of androstenedione included within NaY. More importantly within NaY, similar to cholesteryl acetate the photoreduction product **18** *via* β-hydrogen insertion is obtained as the major product. We believe

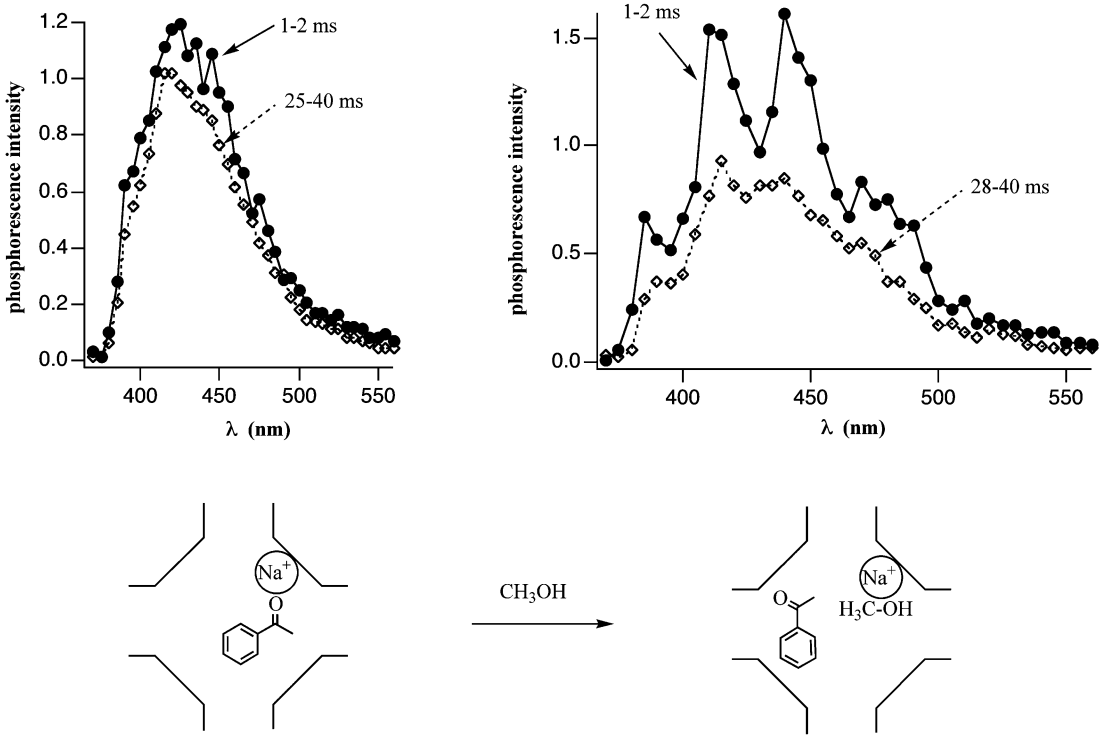

Fig. 10 (left) Time-resolved phosphorescence spectra of acetophenone included in NaY recorded 1–2 ms and 25–40 ms after the lamp pulse (λ_{ex} = 320 nm) at 77 K. (right) Time-resolved phosphorescence spectra of methanol treated acetophenone included in NaY recorded 1–2 ms and 28–40 ms after the lamp pulse (λ_{ex} = 320 nm) at 77 K.

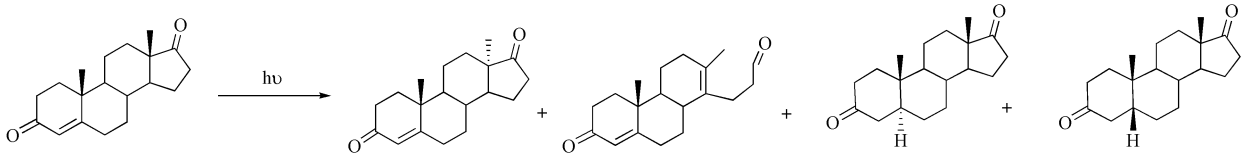

	14	15 (nπ*)	16 (nπ*)	17 (nπ*)	18 (ππ*)
Hexane		40%	4%	–	–
2-Propanol		18	2	14	–
Na Y (Si/Al: 2. 5)		–	–	15	85
High Silica Y (Si/Al: >285)		30 %	–	–	–

Scheme 5

the changes in the reactivity of cholesteryl acetate and androstenedione when included within NaY to be due to the lowering of the ππ* excited state of the cyclohexenone A ring. Enone **11** does not react while enone **14** gives only nπ* derived product **15** in Y–Sil, the zeolite with no cation. These observations emphasize the role of cations in altering the nature of the lowest triplet.

As shown in Scheme 6, of the several products on excitation of 4-methyl-4-phenyl-2-cyclohexenone (**19**), products **23** and

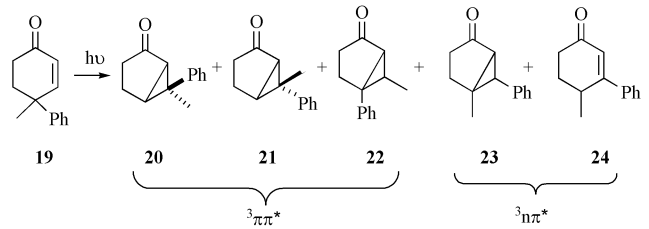

	^{3}ππ*	^{3}nπ*
Benzene	0 %	100%
Ethanol	33	67
NaY/hexane	70	30

Scheme 6

24 have been established to arise from the nπ* triplet and products **20–22** from the ππ* triplet.[16b] Consistent with the behavior of cholesteryl acetate and androstenedione, direct irradiation of enone **19** included within NaY gave higher yields of products **20–22** (70%) derived from the ππ* triplet than in non-polar benzene (0%) or moderately polar ethanol (33%).

Triplet sensitization of 3-methyl-3-(1-cyclopentenyl)butan-2-one (**25**), yields the 1,3-acyl migration product **26** from the nπ* triplet (and nπ* singlet) and the oxa-di-π-methane product **27** from the ππ* triplet (Scheme 7).[16b] The oxa-di-π-methane

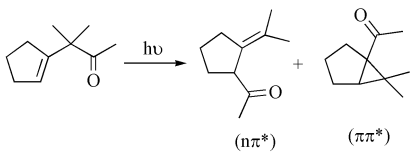

	25	26 (nπ*)	27 (ππ*)
Hexane		100%	0%
Ethanol		78	22
KY/hexane		26	74

Scheme 7

product **27** was obtained in higher yield within zeolite than in non-polar or polar solvents. The selectivity in favor of the ππ* triplet product observed in zeolites once again is consistent with the model that alkali ions lower the ππ* triplet below the nπ* triplet state upon interaction with enones.

Controlling excited state chemistry through alkali metal ion–aromatic-π (quadrupolar) interaction

Direct evidence in favor of alkali metal ion site for the location of benzene, xylenes and mesitylene within NaY based on powder neutron diffraction studies at low temperatures (< 10K) exists.[18] The stability of the alkali metal ion site is believed to be due to cation-π type electrostatic interaction (quadrupolar).[19] Such an interaction most likely plays a role during adsorption of larger aromatic molecules such as naphthalene, phenanthrene and pyrene within zeolites. For example, ^{2}H-NMR spectra of larger aromatic molecules (*e.g.*, phenanthrene-D_{10}) in MX zeolites consist of the two components, narrow and static, where the relative amounts vary with temperature.[20] The heat of dissociation of the ion–phenanthrene complex has been estimated on the assumption that the static component is due to alkali metal ion–phenanthrene bound state and the narrow component to a free state (unbound to alkali metal ions). Supporting the general notion that aromatic molecules interact with the alkali metal ions present in a supercage, a linear relationship between the heat of dissociation and charge density of the alkali metal ion has been observed (enthalpies of interaction: Na^+ −14.9; K^+ −11.0; Cs^+ −7.9 kcal/mol).

In this section we describe a few of the several effects on the excited state behavior of guest molecules resulting from the electrostatic interaction between alkali metal ions and aromatic molecules within zeolites. The role of alkali metal ions during adsorption of aromatic molecules within a zeolite is revealed by the fluorescence spectra of phenanthrene (Fig. 11).[21] Only the

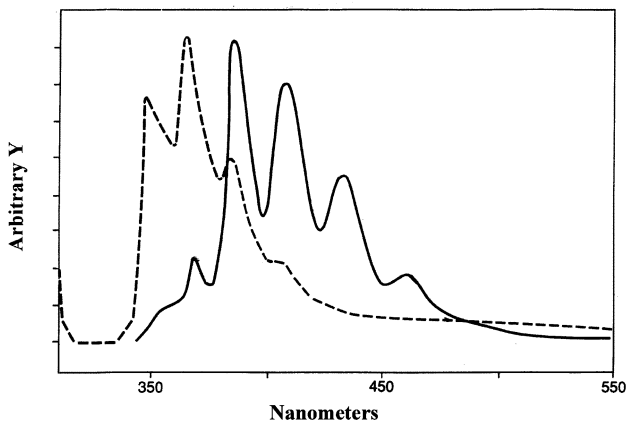

Fig. 11 Fluorescence spectra of phenanthrene, < S > : 0.4, included within "dry" and "wet" NaY: ⋯ "dry" NaY, ex λ: 293 nm; — "wet" NaY, ex λ: 320 nm.

monomer fluorescence is observed upon excitation of phenanthrene included within anhydrous zeolite (one molecule per ten supercages). However, on adsorption of water by the zeolite, in addition to the monomer emission, fluorescence from micro-

crystals is also detected (Fig. 11). The association of phenanthrene to form micro-crystals, we believe, is prompted by the displacement of phenanthrene, by water, from the internal to external surface. We believe that under anhydrous conditions phenanthrene is adsorbed onto the internal surfaces of zeolite through alkali metal ion–arene interaction whereas in a hydrated zeolite, the stronger binding of water molecules to the alkali metal ion displaces the phenanthrene molecules to the outer surface. Consistent with this view dehydration of the hydrated sample led to the complete disappearance of emission due to microcrystals and detection of emission was from the monomer only.

One of the consequences of alkali metal ion coordination to the arene is its polarization such that the open face would attract an electron rich molecule, which in this case is another arene molecule. Computational results strongly support this intuition.[22] The computed alkali metal ion–benzene binding affinities presented in Table 2 (Scheme 8) compare quite well

Table 2 Binding affinities (kcal/mol) computed at MP2 level for $M^+\cdots$benzene$\cdots$benzene system[a]

Metal ion	Structure **28**	Structure **29**	Structure **30**	Structure **31**	Structure **32**	Structure **33**
Li	43.78	48.62	2.08	6.93	81.1	75.8
Na	29.66	33.34	2.08	5.77	56.2	53.9
K	16.74	19.68	2.08	5.03	32.3	32.6
Rb	14.63	17.04	2.08	4.50	27.7	28.2
Cs	11.94	14.04	2.08	4.19	22.6	22.7

[a] See Scheme 8 for description of the structures

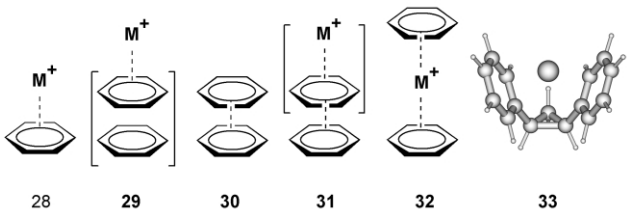

Scheme 8

with the available experimental data.[23] More important in the context of the present study is the prediction that an alkali ion coordinated benzene ring would interact more strongly with a second benzene molecule. The binding affinity of a benzene molecule to a Li^+–complexed benzene ring is as large as 6.9 kcal/mol at the MP2/6-31G* level. Even with the weakly coordinating Cs^+ ion, the corresponding binding affinity is double that of benzene–benzene binding affinity (2.08 kcal/mol) at the same theoretical level. Alkali ion prompted ground state aggregation of arenes is readily detected by excimeric emission of naphthalene, anthracene and pyrene.[22,24] We illustrate this phenomenon below with the photophysical behavior of naphthalene within MY zeolite.[22]

The recorded emission spectrum at room temperature of naphthalene included in 'dry' NaY consists of two components, from monomer and the excimer fluorescence (Fig. 12). The following observations suggest that the latter results from pre-aggregated dimers (static excimers) present within the supercages of NaY. The two emissions have slightly different excitation spectra. No growing-in of the excimer on a nanosecond time scale was noticed when monomer and excimer decays were monitored by time resolved single photon counting. The absence of any negative pre-exponential term for excimer decay also implies that the long wavelength emission is not due to dynamic excimers. Further, the ratio of the excimer to monomer emission increased slightly upon lowering the temperature. Had the broad emission in the region 380–480 nm been due to a dynamic excimer, lowering of the temperature would have resulted in a decrease of the excimer emission. Dynamic excimer formation would require a decrease in

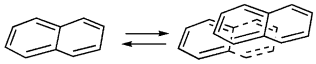

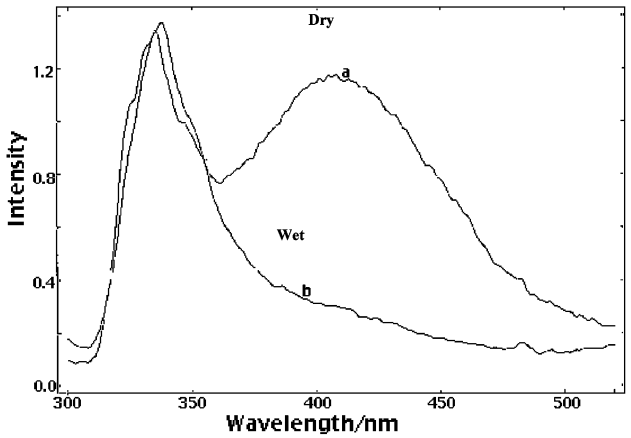

Fig. 12 Fluorescence spectra of naphthalene included within NaY. Dry sample (a) shows both monomer and excimer emissions and the wet sample (b) shows essentially monomer emission.

lifetime with increases in loading level while the static excimer formation would not affect the lifetime at all. Varying the loading level between 0.002 and 0.2 (average number of molecules per supercage) did not alter the naphthalene monomer lifetime significantly. Thus, consistent with the model that the alkali metal ions co-ordinated to water molecules would have lesser polarizing power, the excimer emission can be turned 'on' or 'off' by co-adsorbed water (Fig. 12).

The most energetically stable arrangement of a single alkali ion and two aromatic molecules is the sandwich structure in which the alkali ion is present between the two aromatic molecules (structure **32** in Scheme 8; Table 2). Although the sandwich type of alkali ion binding to two benzene rings is less likely within a zeolite, a predesigned host cavity such as the 'bowl' shaped *cis*-1,2-diphenylcyclopropane (DPC) with optimally poised phenyl rings may be expected to bind to an alkali ion within a zeolite (structure **33** in Scheme 8). *Ab initio* calculations on alkali metal ion complexes with *cis*-DPC reveal that the binding affinities are comparable to those of sandwich structures with free benzene ligands, and are also alkali metal ion-dependent (Table 2).[25] In contrast to *cis*-DPC, in the *trans* isomer the alkali metal ion would bind only to a single benzene ring. This insight allowed us to selectively convert *trans*-DPC **35a** to the *cis* isomer **34a** (Scheme 9). Upon triplet sensitization,

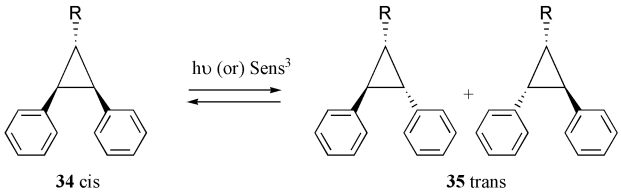

Cis to trans at the photostationary state

	Solution	LiY	NaY	KY
a: R = -H	45:55	95:5	92:8	88:12
b: = -$CONHCH_2CH_2CH_2CH_3$	48:52	12:88	40:60	35:65
c: = -$CONHCH_2Ph$	50:50	11:89	35:65	58:42

Scheme 9

DPC in solution gives a photostationary state consisting of *cis* and *trans* isomers in the ratio 45:55. However, within NaY upon triplet sensitization the photostationary state was enriched with the cis isomer up to 92%.

In the bowl type structure **33** any motion disrupting the co-operative interaction of the alkali metal ion to the two phenyl groups would be resisted both in the ground and excited states.

Since conversion from the *cis* geometry to the *trans via* 1,3-diradical intermediate involves such a disruption, this process is expected to have a barrier in the excited state within a zeolite. Consistent with the postulate that the alkali metal ion is most important for the *cis* enrichment within zeolites, inclusion of water (a better co-ordinator to the alkali ion) within LiY resulted in a photostationary state similar to that in solution (*cis*:*trans*, 49:51). Further, the *cis*:*trans* ratio in Cs^+ which has small interaction energy (Table 2) gives much less *cis* (CsY: 65%) in the photostationary state than Li^+ (LiY: 95%).

If the above model is correct, isomerization from the *cis* to the trans geometry should be possible in systems with preferential binding of the alkali metal ion to a site other than the *cis*-diphenyl groups. The photobehavior of the amides of 2β,3β-diphenylcyclopropane-1α-carboxylic acid (**34/35b** and **34/35c**; Scheme 9) is consistent with this expectation.[26] For example the alkyl amides of 2β,3β-diphenylcyclopropane-1α-carboxylic acid upon triplet sensitization within NaY gave both trans and cis isomers similar to that in solution (Scheme 9). Computational (B3LYP/6-31G*) results on methyl amide of 2β,3β-diphenylcyclopropane-1α-carboxylic acid provide an insight into the excited state behavior of the above molecules. Computation suggested the possibility of three structures of nearly equal binding affinities in which the alkali metal ion bound either solely to the amide or co-operatively to the amide and the phenyl groups or to the two phenyl groups of methyl amide of 2β,3β-diphenylcyclopropane-1α-carboxylic acid (Fig. 13). No barrier for rotation of cis to the trans geometry is expected in Structure-1 and Structure-3 shown in Fig. 13.

Exploitation of alkali metal ion–diphenyl co-operative binding to control photoproduct distributions is further exemplified by the excited state chemistry of benzyl aryl ethers. For example, photolysis of benzyl phenyl ether **36** in hexane results in the formation of four products (**37–40**) in nearly equal amounts *via* cleavage of the benzyl–ether oxygen bond (Scheme 10).[22] On the other hand, irradiation of benzyl phenyl ether included in NaY gave *ortho*-benzyl phenol **39** as the major product. According to computation (B3LYP/6-31G*) a sandwich-type structure shown in Fig. 14 is preferred by the Li^+–benzyl phenyl ether complex. Upon irradiation of the above sandwich type Li^+ complex, the two fragments of the molecule resulting from benzyl–oxygen bond cleavage would be subjected to translational and rotational restrictions by the alkali metal ion. While in solution the two fragments would be free to diffuse to yield *ortho* and *para* rearranged products, within zeolites the metal ion would hold and direct them to a product requiring least motion, namely the *ortho* isomer **39**. As recognized during the photo-Fries rearrangements of phenyl acetate, phenyl benzoate, acetanilides and naphthyl esters, selectivity can occur even when two interacting groups are not aryl groups.[27,28] In these examples, the alkali metal ion binding co-operatively to aryl and ester/amide groups leads them to the *ortho* rearranged products.

The most impressive example is provided by the photo-Fries rearrangement of 1-naphthyl phenyl acylate **41** (Scheme 11).[29] This molecule resulting in eight products (**42–49**) upon irradiation in hexane solution yields a single product **42** within NaY zeolite. We believe the cage effect provided by the confined medium and the rotational restriction enforced by the aromatic-alkali ion-ester interaction favor the *ortho* coupling of the primary radical pair even before decarbonylation can occur. The three modes of interaction of Li^+ to 1-naphthyl phenyl

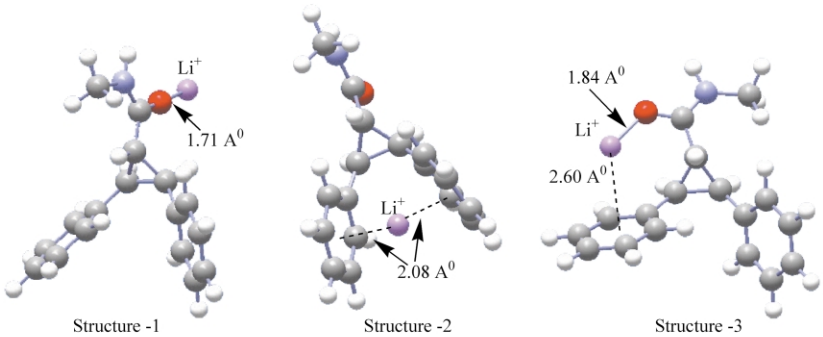

Binding Affinity (kcal/mol)

Cation	Structure -1	Structure -2	Structure -3
Li^+	64.13	64.82	67.96
Na^+	46.75	47.75	50.01
K^+	33.63	32.88	34.76

Fig. 13 B3LYP/6-31G* optimized geometries of complexes of Li^+ ion with methyl amide of 2β,3β-diphenylcyclopropane-1α-carboxylic acid. Binding affinities with Li^+, Na^+ and K^+ are also included. Note the difference in the location of cation in the three structures. The three structures have almost the same energy.

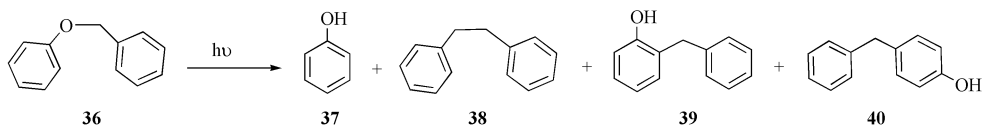

36 **37** **38** **39** **40**

Hexane	28	16	30	26
NaY	7	-	85	10

Scheme 10

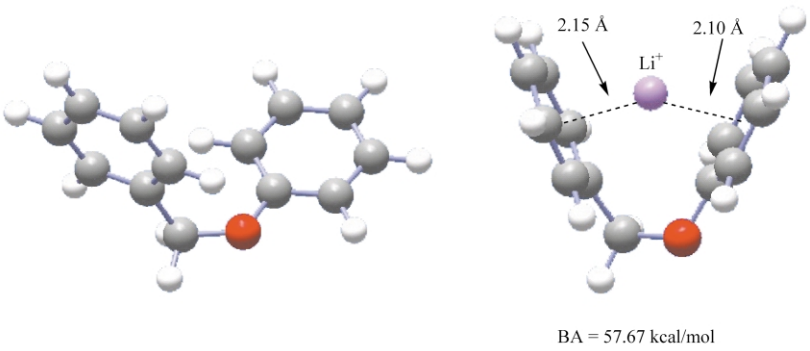

Fig. 14 B3LYP/6-31G* optimized geometries of benzyl phenyl ether and its complex with Li^+. Binding affinity for the later complex indicated on the bottom.

acylate possessing similar binding affinities are shown in Fig. 15. A feature common to all three structures is the co-operative binding of the alkali metal ion to two parts of the molecule that would enforce restrictions on the two fragments resulting from photocleavage of the naphthoxy and carbonyl bond. Under such conditions *ortho* rearrangement would be favored.

The final example concerns the photolysis of α-alkyldeoxybenzoin **50** (Scheme 12).[30] This molecule upon irradiation in solution gives products of Norrish type I and type II processes with the latter being the major one. On the other hand, within MY zeolites Norrish type I products (**51–53**) are favored over the Norrish type II products **54** and **55** (Scheme 12). The Norrish type II reaction requiring a conformation in which the γ-hydrogen approaches the carbonyl oxygen along the n-orbital is preferred in solution (Fig. 16). As seen in Fig. 16, Li^+ through co-operative interaction with the phenyl and carbonyl groups of α-alkyldeoxybenzoins holds the molecule in a conformation where the γ-hydrogen abstraction could reach the carbonyl only along the π-face that would not result in hydrogen abstraction. Thus the switch in the conformational preference enforced by

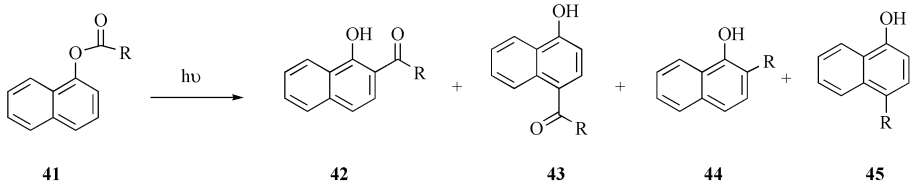

R = -CH_2Ph	Hexane	43%	15	9	11
	NaY	97%	3	-	-

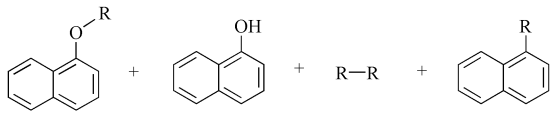

Hexane	2%	14	5	2
NaY	-	-	-	-

Scheme 11

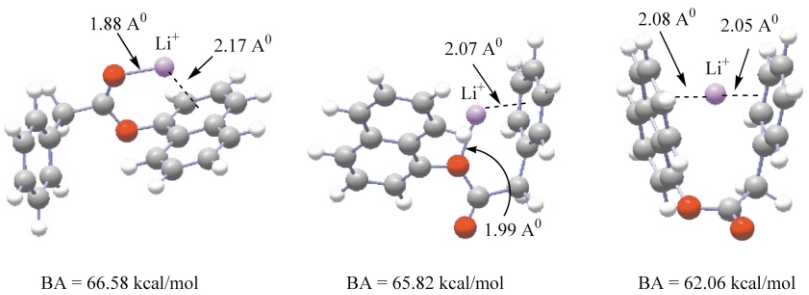

Fig. 15 B3LYP/6-31G* optimized geometries and binding affinities of Li^+ complex with 1-naphthyl phenyl acylate .

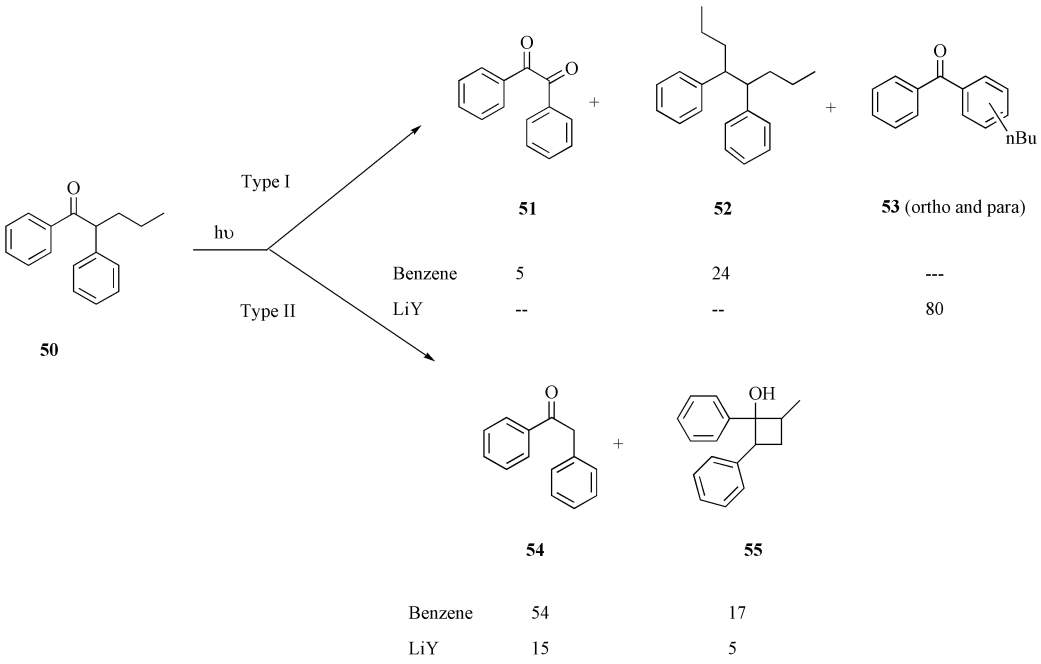

Scheme 12

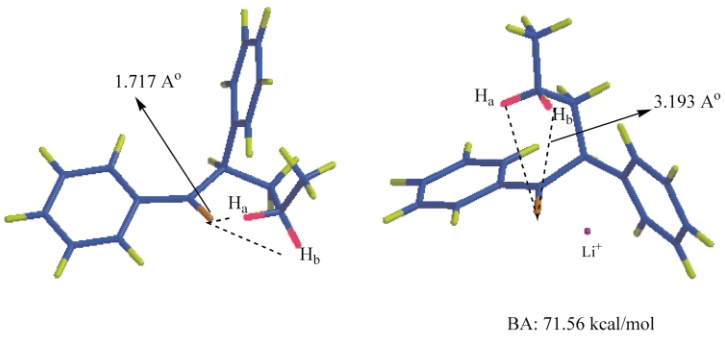

Fig. 16 HF/6-31G* optimized geometries of α-propyl deoxybenzoin and its complex with Li^+.

the alkali ion turns off the generally favored Norrish type II process.

Controlling excited state chemistry through alkali metal ion–olefin-π (quadrupolar) interaction

Computed binding affinities of alkali metal ions to two representative olefins listed in Fig. 17 show a interaction.[31] As seen with 5-phenyl-2-methyl-2-pentene, the presence of an aryl substituent strengthens binding through co-operative interaction between the metal ion and olefin and aryl groups. In both the structures Li^+ is shifted towards the less substituted side of the olefin (compare the distance between Li^+ and C_1 and C_5 in the case of 2-methyl-2-butene and between Li^+ and C_1 and C_{12} in the case of 5-phenyl-2-methyl-2-pentene. Further, the ion is much closer to the less substituted olefinic carbon (compare the distance between Li^+ and C_1 and C_2). At the HF/6-31G** level, an interesting orbital polarization is seen for the Li^+–2-methyl-2-butene complex (Fig. 18). The π HOMO lobes of the olefin are relatively larger on the less substituted olefin center. The above differences in the electronic and structural characteristics between free and alkali ion bound olefins suggested that the nature of the electrophilic addition of singlet oxygen to trisubstituted olefins would be different within zeolites.

It has been established that singlet oxygen adds to a trisubstituted olefin (with three α-hydrogens) from the more substituted side and yields equal amounts of both secondary and tertiary hydroperoxides (Scheme 13).[32] Based on the structural data presented in Fig. 17, the alkali ion complexed olefin may be expected to be attacked by the singlet oxygen from the less substituted side (the electrophilic addition would be steered by M^+ which is present on the less substituted side; Fig. 17) to form an initial interaction with the carbon (C_2) with less substitution and higher electron density (Fig. 18). Such an addition would lead to hydrogen abstraction from the terminal methyl groups leading to the secondary hydroperoxide at the expense of the tertiary hydroperoxide, *i.e.*, the non-selective reaction would become selective within zeolites. Results presented for the two olefins **56** and **59** in Scheme 13 indicate that our expectations have been realized.[31,33] Although the details of the mechanism are still being debated, following our initial suggestion, several groups agree on the importance of alkali ion binding to olefins during singlet oxygen oxidation within zeolites.[34] Consistent with the model assigning selectivity to alkali ion binding, the yield of the secondary hydroperoxide decreases when the stronger binding Li^+ is replaced with weaker binding Cs^+ in zeolites (Scheme 13).

Summary and outlook

During the past three decades a number of organized assemblies (molecular crystals, inclusion complexes in the solid state as well as in solution, liquid crystals, micelles and related assemblies, monolayers, LB films, surfaces and natural systems such as DNA) have been examined as media in controlling the excited state behavior of organic molecules.[1,35] Zeolites are versatile with superior ability in controlling reactions of a large

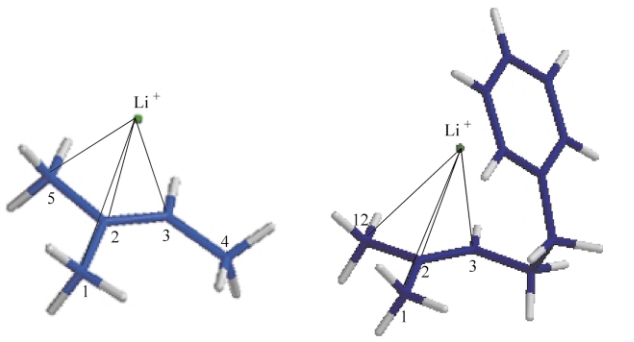

$Li-C_3$	$Li-C_2$	$Li-C_1$	$Li-C_5$	$Li-C_3$	$Li-C_2$	$Li-C_1$	$Li-C_{12}$
2.31	2.24	3.28	2.39 A^0	2.36	2.64	3.61	3.12 A^0

Metal Ion	Binding Affinity (kcal/mol)	
	2-methyl-2-butene	5-phenyl-2-methyl-2-pentene
Li^+	31.3	56.8
Na+	21.5	40.2
K+	11.1	16.4
Rb+	8.9	11.9
Cs+	6.4	7.5

Fig. 17 Calculated (B3LYP/6-31G*) key Li^+–carbon distances of Li^+ complexes (left) of 2-methyl-2-butene and (right) 5-phenyl-2-methyl-2-pentene. Binding affinities are provided below the structures.

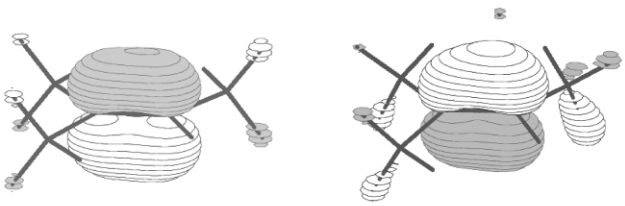

Fig. 18 The π-HOMO of 2-methyl-2-butene (left) and its Li+ complex (right) calculated at HF/6-31G* level.

variety of molecules.[36] Our recognition of the non-passive nature of the zeolite cavity has helped us control photoprocesses of included organic molecules. The examples presented in this article demonstrate the possibility for controlling the excited state behavior of organic molecules through exploitation of the alkali ions present in zeolites.

To understand the remarkable variations in excited state processes within zeolites we have employed *ab initio* computations on model systems.[37,38] Such calculations corroborate the attribution of many of the observed general features to structural and excited state energetic changes induced by cation-organic interactions. Deeper understanding of the influence of cations on excited state behavior of organic molecules and accurate predictions necessarily require careful accounting of the zeolite environment which dictates precise structural characterization of the guest within it.[39] Our results have revealed that alkali cations of zeolites can be used to control excited state reactions where the zeolites control on selectivity may only be the provision of an appropriate scaffold with partially solvated and co-ordinated cations for interaction with the organic substrate. Perhaps similar selectivities may then be achieved in solution phase by incomplete solvation of alkali cations in organic solvents. We hope to see developments in this direction in the coming years.

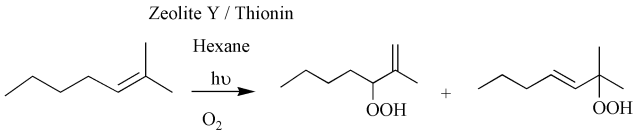

Medium	57	58
Acetonitrile/RB	49	51
LiY / Thionin	74	26
NaY / Thionin	74	26
RbY / Thionin	59	41
CsY / Thionin	50	50

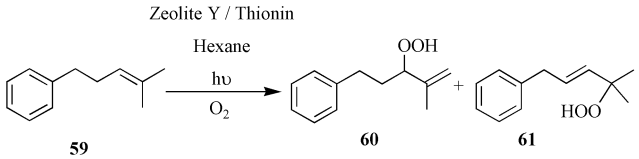

Cation	60	61
Acetonitrile /RB	53	47
LiY / Thionin	95	5
NaY / Thionin	88	12
RbY / Thionin	70	30
CsY / Thionin	52	48

Scheme 13

Examples provided above bring out the remarkable similarity between enzymes and zeolites.[5] Recent examples of thermal reactions within zeolites provided by Thomas, Harris and co-workers further support the above view.[40] Zeolites similar to enzymes provide a confined space and an active site (alkali ion) where a molecule could be manipulated. Zeolites are far more versatile and unique to be only used as shape-selective catalysts.

Acknowledgement

VR thanks M. Warrier, P. H. Lakshminarasimhan, S. Uppili, J. Sivaguru, S. Karthikeyan, K. Pitchumani, V. Jayathirtha Rao, K. J. Thomas, S. Takagi, A. Pradhan and S. Jockusch for their intellectual and experimental contributions, and the National Science Foundation (CHE-9904187 and CHE-0212042), Department of Energy and Petroleum Research Foundation for support of the research summarized here. It is a pleasure for VR to acknowledge the valuable collaborations with N. J. Turro, R. G. Weiss, J. R. Scheffer and L. J. Johnston.

Notes and references

1 (*a*) *Photochemistry in Organized and Constrained Media*, V. Ramamurthy (Ed.), VCH: New York, 1991; (*b*) H. Dodziuk, *Introduction to Supramolecular Chemistry*, Kluwer Academic Publishers: Dordecht, 2002.

2 (*a*) M. D. Cohen, *Angew. Chem., Int. Ed. Engl.*, 1975, **14**, 386; (*b*) R. G. Weiss, V. Ramamurthy and G. S. Hammond, *Acc. Chem. Res.*, 1993, **26**, 530.

3 P. B. Weisz, *Pure & Appl. Chem.*, 1980, **52**, 2091.
4 D. W. Breck, *Zeolite Molecular Sieves: Structure, Chemistry and Use*, John Wiley and Sons, New York, NY, 1974. Ch. 8.
5 (*a*) J. M. Thomas, *Angew. Chem. Int. Ed. Engl.*, 1988, **27**, 1673; (*b*) J. M. Thomas, *Angew. Chem. Int. Ed. Engl.*, 1994, **33**, 913; (*c*) J. M. Thomas and R. Raja, *Chem. Commun.*, 2001, 675; (*d*) N. Herron, *Chemtech*, 1989, **19**, 542.
6 D. W. Breck, *Zeolite Molecular Sieves: Structure, Chemistry and Use*, John Wiley and Sons, New York, NY, 1974.
7 N. J. Turro, *Modern Molecular Photochemistry*, University Science Books, Mill Valley, CA, 1991.
8 (*a*) V. Ramamurthy, J. V. Caspar, D. R. Corbin and D. F. Eaton, *J. Photochem. Photobiol., A: Chemistry.*, 1989, **50**, 157; (*b*) J. V. Caspar, V. Ramamurthy and D. R. Corbin, *Coord. Chem. Rev.*, 1990, **97**, 225; (*c*) V. Ramamurthy, J. V. Caspar and D. R. Corbin, *Tetrahedron Letters*, 1990, **31**, 1097; (*d*) V. Ramamurthy, J. V Caspar, E. W. Kuo, D. R. Corbin and D. F. Eaton, *J. Am. Chem. Soc.*, 1992, **114**, 3882.
9 V. Ramamurthy, J. V Caspar, D. R. Corbin, B. D. Schlyer and A. H. Maki, *J. Phys. Chem.*, 1990, **94**, 3391.
10 S. Uppili, V. Marti, A. Nikolaus, W. Adam, P. S. Engel, N. J. Turro and V. Ramamurthy, *J. Am. Chem. Soc.*, 2000, **122**, 11025.
11 V. Ramamurthy, D. R. Corbin, C. V. Kumar and N. J. Turro, *Tetrahedron Letters*, 1990, **31**, 47.
12 K. Pitchumani, M. Warrier, V. Ramamurthy and J. R. Scheffer, *Chem. Commun.*, 1998, 1197.
13 M. Warrier, N. J. Turro and V. Ramamurthy, *Tetrahedron Letters*, 2000, **41**, 7163.
14 J. Shailaja, P. H. Lakshminarasimhan, A. Pradhan, R. B. Sunoj, S. Jockusch, S. Karthikeyan, S. Uppili, J. Chandrasekhar, N. J. Turro and V. Ramamurthy, *J. Phys. Chem. A.*.
15 R. B. Sunoj, P. Lakshminarasimhan, V. Ramamurthy and J. Chandrasekhar, *J. Comput. Chem.*, 2001, **22**, 1598.
16 (*a*) V. Jayathirtha Rao, S. Uppili, D. R. Corbin, S. Schwarz, S. R. Lustig and V. Ramamurthy, *J. Am. Chem. Soc.*, 1998, **120**, 2480; (*b*) S. Uppili, S. Takagi, R. B. Sunoj, P. Lakshminarasimhan, J. Chandrasekhar and V. Ramamurthy, *Tetrahedron Letters.*, 2001, **42**, 2079.
17 (*a*) D. I. Schuster, J. Woning, N. A. Kaprinidis, Y. Pan, B. Cai, M. Barra and C. A. Rhodes, *J. Am. Chem. Soc.*, 1992, **114**, 7029; (*b*) A. C. Chan and D. I. Schuster, *J. Am. Chem. Soc.*, 1986, **108**, 4561.
18 (*a*) A. N. Fitch, H. Jobic and A. Renouprez, *Chem. Commun.*, 1985, 284; (*b*) R. Goyal, A. N. Fitch and H. Jobic, *Chem. Commun.*, 1990, 1152.
19 (*a*) J. C. Ma and D. A. Dougherty, *Chem. Rev.*, 1997, **97**, 1303; (*b*) G. W. Gokel, S. L. De Wall and E. S. meadows, *Eur. J. Org. Chem.*, 2000, 2967; (*c*) G. W. Gokel, L. J. Barbour, R. Ferdani and J. Hu Jiax, *Acc. Chem. Res.*, 2002, **35**, 878.
20 M. A. Hepp, V. Ramamurthy, D. R. Corbin and C. Dybowski, *J. Phys. Chem.*, 1992, **96**, 2629.
21 V. Ramamurthy, *Mol. Cryst. Liq. Cryst.*, 1994, **240**, 53.
22 K. J. Thomas, R. B. Sunoj, J. Chandrasekhar and V. Ramamurthy, *Langmuir*, 2000, **16**, 4912.
23 J. B. Nicholas, B. P. Hay and D. A. Nixon, *J. Phys. Chem.*, 1999, **103**, 1394.
24 (*a*) V. Ramamurthy, D. F. Eaton and D. R. Sanderson, *J. Phys. Chem.*, 1993, **97**, 13380; (*b*) S. Hashimoto, S. Ikuta, T. Asahi and H. Masuhara, *Langmuir*, 1998, **14**, 4284; (*c*) K. K. Iu and J. K. Thomas, *Langmuir*, 1990, **6**, 471.
25 P. Lakshminarasimhan, R. B. Sunoj, J. Chandrasekhar and V. Ramamurthy, *J. Am. Chem. Soc.*, 2000, **122**, 4815.
26 L. S. Kaanumalle, J. Sivaguru, P. H. Lakshminarasimhan, R. B. Sunoj, J. Chandrasekhar and V. Ramamurthy, *J. Org. Chem.*, 2002, **67**, 8711.
27 W. Gu, M. Warrier, B. Schoon, V. Ramamurthy and R. G. Weiss, *Langmuir*, 2000, **16**, 6977.
28 (*a*) K. Pitchumani, M. Warrier and V. Ramamurthy, *J. Am. Chem. Soc.*, 1996, **118**, 9428; (*b*) K. Pitchumani, M. Warrier, C. Cui, R. G. Weiss and V. Ramamurthy, *Tetrahedron Letters*, 1996, **37**, 6251; (*c*) K. Pitchumani, M. Warrier and V. Ramamurthy, *Res. Chem. Intermediates*, 1999, **25**, 623.
29 W. Gu, M. Warrier, V. Ramamurthy and R. G. Weiss, *J. Am. Chem. Soc.*, 1999, **121**, 9467.
30 (*a*) D. R. Corbin, D. F. Eaton and V. Ramamurthy, *J. Am. Chem. Soc.*, 1988, **110**, 4848; (*b*) D. R. Corbin, D. F. Eaton and V. Ramamurthy, *J. Org. Chem.*, 1988, **53**, 5384.
31 J. Shailaja, J. Sivaguru, R. J. Robbins, V. Ramamurthy, R. B. Sunoj and J. Chandrasekhar, *Tetrahedron*, 2000, **56**, 6927.
32 H. H. Wasserman, R. W. Murray (Eds.), *Singlet Oxygen*, Academic Press, New York, 1979.
33 (*a*) X. Li and V. Ramamurthy, *J. Am. Chem. Soc.*, 1996, **118**, 10666; (*b*) R. Robbins and V. Ramamurthy, *J. Chem. Soc. Chem. Commun.*, 1997, 1071; (*c*) L. S. Kaanumalle, J. Shailaja, R. J. Robins and V. Ramamurthy, *J. Photochem. Photobiol A: Chemistry*, 2002, **153**, 55.
34 (*a*) E. L. Clennan, J. P. Sram, A. Pace, K. Vincer and S. White, *J. Org. Chem.*, 2002, **67**, 3975; (*b*) A. Pace and E. L. Clennan, *J. Am. Chem. Soc.*, 2002, **124**, 11236; (*c*) M. Stratakis and G. Kosmas, *Tetrahedron Letters*, 2001, **42**, 6007; (*d*) G. Froudakis and M. Stratakis, *Eur. J. Org. Chem.*, 2003, 359.
35 V. Ramamurthy, R. G. Weiss and G. S. Hammond, *Adv. Photochem.*, 1993, **18**, 67.
36 (*a*) V. Ramamurthy, D. F. Eaton and J. V Caspar, *Acc. Chem. Res.*, 1992, **25**, 299; (*b*) V. Ramamurthy, P. Lakshminarasimhan, C. P. Grey and L. J. Johnston, *Chem. Comm.*, 1998, 2411; (*c*) J. Sivaguru, N. Arunkumar, L. S. Kaanumalle, J. Shailaja, S. Uppili, A. Joy and V. Ramamurthy, *Acc. Chem. Res.*, 2003, in press.
37 All the calculations were carried out using Gaussian98 series of programs.M. J. Frisch, *et al.*, *Gaussian 98, Revision A. 6*; Gaussian, Inc.: Pittsburg, PA, 1998.
38 (*a*) M. E. Casida, C. Jamorski, K. C. Casida and D. R. Salahub, *J. Chem. Phys.*, 1998, **108**, 4439; (*b*) A. D. Becke, *Phys. Rev. A.*, 1988, **38**, 3098; (*c*) C. Lee, W. Yang and R. G. Parr, *Phys. Rev. B.*, 1988, **37**, 785; (*d*) M. Casida, In *Recent Advances in Density Functional Methods*: D. P. Chong, Ed., World Scientific Press: Singapore, 1995, **Vol I**. p. 155.
39 *Modelling of Structure and Reactivity in Zeolites*, C. R. A. Catlow (ed.), Academic Press: London, 1992.
40 (*a*) S. O. Lee, S. J. Kitchin, K. D. M. Harris, G. Sankar, M. Dugal and J. M. Thomas, *J. Phys. Chem. B.*, 2002, **106**, 1322; (*b*) S. O. Lee, G. Sankar, S. J. Kitchin, M. Dugal, J. M. Thomas and K. D. M. Harris, *Catalysis Letters.*, 2001, **73**, 91; (*c*) J. M. Thomas, R. Raja, G. Sankar and R. G. Bell, *Nature*, 1999, **398**, 227.